Molecular Catalysis 497 (2020) 111200

Contents lists available at ScienceDirect

Molecular Catalysis

journal homepage: www.journals.elsevier.com/molecular-catalysis

Pd-Nanoparticles immobilized organo-functionalized SBA-15: An efficient heterogeneous catalyst for selective hydrogenation of C—C double bonds of α,β-unsaturated carbonyl compounds

Anand Narani [a,c,d,*], Hari Prasad Reddy Kannapu [c], Kishore Natte [b,d], David Raju Burri [c,**]

[a] Biofuels Division, CSIR-Indian Institute of Petroleum, Haridwar Road, Mohkampur, Dehradun, 248005, Uttarakhand, India
[b] Chemical and Material Sciences Division, CSIR-Indian Institute of Petroleum, Haridwar Road, Mohkampur, Dehradun, 248005, Uttarakhand, India
[c] Catalysis Laboratory, I&PC Division, Indian Institute of Chemical Technology, Hyderabad, 500 007, India
[d] Academy of Scientific and Innovative Research (AcSIR), Sector 19, Kamla Nehru Nagar, Ghaziabad, Uttar Pradesh, 201 00, India

ARTICLE INFO

Keywords:
SBA-15
Anchoring
Palladium nanoparticles
Selective hydrogenation
High TOF

ABSTRACT

A novel PdNPs/SBA-NH_2-LA catalyst has been prepared by a post-synthetic grafting approach *via* successive anchoring of propylamine (SBA-NH_2) and lipoic acid (SBA-NH_2-LA) functional groups followed by palladium nanoparticles immobilization. The Physico-chemical properties of the catalyst were extensively investigated by XRD, N_2 adsorption-desorption, XPS, FT-IR, and TEM analysis. The PdNPs/SBA-NH_2-LA catalyst is found to be highly selective for the hydrogenation of C—C double bonds of α, β-unsaturated carbonyl compounds. Excellent conversion (95–99 %) and selectivity (>99 %) with high turn over frequency (330−1065 h^{-1}) achieved at room temperature under atmospheric hydrogen pressure within 30−90 min of reaction time. This kind of high activity is expected from its structural and textural integrity of the catalyst.

Introduction

Hydrogenation is a key step in the industry for the synthesis of fine chemicals, fuels, and drug molecules. [1–7] Among several hydrogenation reactions, chemoselective hydrogenation of C—C double bonds of α, β-unsaturated carbonyl compounds received enormous interest in the fields of academia and industry because, the corresponding saturated aldehydes/ketones have broad applications in food, fragrance, and cosmetic industries. [8–10] Also, the hydrogenated products serve as important intermediates for the preparation of biologically active molecules. [11,12]

Considering the thermodynamics, competing for C═O, aromatic ring hydrogenation, and deoxygenation reactions, the chemoselective hydrogenation of C—C double bonds of α, β-unsaturated carbonyl compounds is still remained as a challenging task. [13] In this respect, numerous homogeneous metal complexes such as Ru [14,15], Rh [16, 17], Pt [18], Ir [19–21], Pd [22,23], Ti [24] [25], Mo [26], Cu [27,28], and Fe [29] have been employed for the selective hydrogenation of C—C double bonds of α, β-unsaturated carbonyl compounds. They exhibit high conversion with excellent selectivity. However, these homogeneous systems have severe drawbacks like catalyst separation and reusability, which leads to the generation of large amounts of waste and at the same time, manufacturing process will become costly. With commercially available Pd/C catalyst, chemoselectivity was the major problem [4]. To avoid these issues, Crooks [30], Kim [31], Ondruschka [32], Stolle [33], Bhanage [34,35], Kantam [36], David [37], Mallick [38], Shen [39] and others [40,41] [42–45], have developed supported Pd nanoparticles and used for hydrogenation of C—C double bonds of α, β-unsaturated carbonyl compounds in different reaction conditions. Also, Au supported on mesostructured CeO_2 catalyst reported for hydrogenation of α, β-unsaturated carbonyl compounds. [46] However, this catalytic system was targeted for C═O bond hydrogenation rather than the C═C bond. Recently, Cu nanoparticles supported on silica catalyst reported for selective hydrogenation of α, β-unsaturated carbonyl compounds in Toulene solvent. [47] Although the catalyst displays an excellent catalytic activity and selectivity but intolerant to a few functional groups and requires high pressures. Very recently, Yang et al., developed biomass derived cobalt nanoparticles for chemoselective hydrogenation of α, β-unsaturated carbonyl compounds in a water solvent. [48] The catalyst exhibits an excellent activity and

* Corresponding author at: Biofuels Division, CSIR-Indian Institute of Petroleum, Haridwar Road, Mohkampur, Dehradun, 248005, Uttarakhand, India.
** Corresponding author.
E-mail address: anand.narani@iip.res.in (A. Narani).

https://doi.org/10.1016/j.mcat.2020.111200
Received 7 January 2020; Received in revised form 28 August 2020; Accepted 30 August 2020
Available online 30 September 2020

afforded 61–97 % yields of C═C bond hydrogenated products. Despite its remarkable activity and selectivity, the catalysts require high pressures and long reaction times.

On the other hand, mesoporous silica materials have recently garnered interest as a catalytic supports due to their fascinating physical and chemical properties. [49,50] Among the availability of various mesoporous silica materials, hexagonally ordered mesoporous SBA-15 display excellent exceptional properties such as high surface area, thermal, hydrothermal stability, thick pore walls, and larger and uniform pore size, which can provide the ideal environment to grow the metal nanoparticles inside the pores of SBA-15 [51–54]. The deposition of Pd nanoparticles into the pores of SBA-15 can be achieved by conventional methods. However, leaching of the active metal centers into the reaction media is a severe problem from an industrial perspective. In contrast, the immobilization of active metal sites by using organic functional groups between SBA-15 and active metal centers has emerged as an efficient method to prepare small and isolated metal nanoparticles with a narrow distribution [55–60]. Furthermore, these organo-functionalized materials will provide synergistic properties of both organic moiety and porous structure, such as versatile functionalization ability for immobilization of active sites, high surface area, and structural stability [61]. Additionally, these materials also act as heterogeneous catalysts to overcome the leaching problems associated with conventional preparation methods. Recently, Esmail et al. reported organofunctionalized mesoporous silica materials along with the deposition of metal nanoparticles for a wide variety of oxidation reactions. These catalysts are highly active and selective for the corresponding products. Moreover, these catalysts are easily recoverable and reusable for numerous cycles. [50,62–64]

Herein, for the first time, we demonstrate a novel method for the preparation of finely dispersed Pd nanoparticles on lipoic acid functionalized SBA-15 (PdNPs/SBA-NH_2-LA). The catalyst is highly stable and reusable for chemoselective hydrogenation of C—C double bonds of α, β-unsaturated carbonyl compounds (Scheme 1).

Experimental

Materials and instrumentation

Unless otherwise stated, all chemicals are purchased from Sigma-Aldrich and used as received. Low-angle XRD patterns were recorded on Ultima IV X-ray diffractometer at 40 kV and 40 mA using CuK_α radiation over the range 0.7_ 6 2h 6 5.0. Wide-angle X-ray diffraction (XRD) patterns of catalysts were obtained on a Bruker D8 Advance X-Ray Powder Diffractometer using Ni filtered Cu Ka radiation at a scan speed of 2° min-1. X-ray photoelectron spectroscopy (XPS) analysis of the catalyst was carried out by a Kratos analytical spectrophotometer, with Mg Ka monochromated excited radiation (1253.6 eV). The residual pressure in the analysis chamber was around 10−9m bar. The binding energy (BE) measurements were corrected for charging effects concerning the C 1s peak of the adventitious carbon (284.6 eV). Infrared spectra were recorded on a Bruker Alpha-T, FT-IR system, in the scan range of 4000–400 cm^{-1}. A Philips Tecnai F12 FEI transmission electron microscope (TEM) operating at 80–100 kV was used to record TEM images.

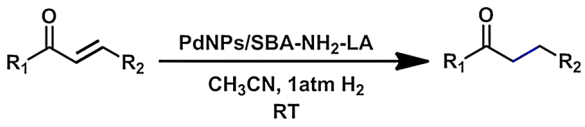

Scheme 1. Selective hydrogenation of C—C double bonds of α,β-unsaturated carbonyl compounds over PdNPs/SBA-NH_2-LA catalyst.

Preparation of catalyst

Preparation of PdNPs/SBA-NH_2-LA catalyst

Pd-Nanoparticles immobilized on lipoic acid functionalized SBA-15 has been synthesized as per the reported procedure [55], and the details are shown in Scheme 2. Initially, the mesostructured parent SBA-15 was synthesized using P123 triblock copolymer surfactant (EO20-PO70-EO20, Aldrich, USA) as a structure-directing agent, tetraethylorthosilicate as silica resource using the hydrothermal process under acidic conditions with EO20PO70EO20:2 M HCl: TEOS: H_2O = 2:60:4.25:15 ratio. At last, the template free SBA-15 is obtained by calcination at 550 °C for 6 h, and it has been used as catalyst support. The amine-functionalized SBA-15 (SBA-NH_2) was prepared by immobilizing 3-(Aminopropyl)triethoxysilane (APTES) on pre-treated template free SBA-15 in toluene under N_2 atmosphere at reflux temperature. Later, the lipoic acid (LA) has been anchored onto SBA-NH_2 (SBA-NH_2-LA) using an amide coupling agent (1-Hydroxy benzotriazole (HOBT) and EDC (lipoic acid: HOBT: EDC at 1:1.1:1.5) in dichloromethane at room temperature for 24 h under an inert atmosphere. Finally, Pd nanoparticles immobilized on lipoic acid-functionalized SBA-15 achieved by reducing the Palladium acetate in methanol solution using $NaBH_4$ under the N_2 atmosphere at room temperature overnight. The resulted catalyst is designated as PdNPs/SBA-NH_2-LA.

Catalytic activity

All hydrogenation reactions were carried out in a 25 mL round bottom flask. In a typical experiment, 1 mmol of the substrate was dissolved in 3 mL solvent, added 10 mg of catalyst to the reaction mixture, and continuously stirred at room temperature under 1 atm H_2 atmosphere (hydrogen balloon) for a required time. After completion of the reaction, the catalyst was separated using simple filtration and washed with acetone followed by drying. The products were analyzed and identified by GC–MS (QP-5050 model, M/s. Shimadzu Instruments, Japan) equipped with ZB-5 capillary column (0.32 mm diameter and 25 m long, supplied by M/s. J & W Scientific, USA).

Results and discussion

As shown in Scheme 2, the PdNPs/SBA-NH_2-LA catalyst was synthesized in three steps. The loading of propylamine, lipoic acid functional groups, and PdNPs are determined by C, H, N, S, and ICP-MS analysis. The propylamine loading was 2.0 mmol/g, and lipoic acid was 0.6 mmol/g. The Pd content was determined to be 1.96 wt%.

Catalyst characterization

N_2 adsorption-desorption analysis

The structure and textural properties of SBA-15, SBA-NH_2, SBA-NH_2-LA, and PdNPs/SBA-NH_2-LA are determined by N_2 adsorption-desorption analysis, and the corresponding isotherms are displayed in Fig. 1. All four samples exhibit type-IV isotherm with H1 hysteresis loop, [65,66] representing the intact of the ordered mesoporous structure of parent SBA-15 after the successive functionalization of propylamine, lipoic acid groups, and deposition of Pd nanoparticles. Inset (Fig. 1) shows the pores are distributed between 4.6–7.10 nm. The BET surface area of SBA-15 is 713 m^2/g, and a decrease in the surface area (429 m^2/g) was observed after successive functionalization with propylamine and lipoic acid. Further, the BET surface area is reduced to 398 m^2/g after the immobilization of Pd nanoparticles. A similar trend was monitored in the case of pore volume and pore diameter, indicating the partial blockage of pores by the introduction of propylamine, lipoic acid groups, and Pd nanoparticles on the surface of the parent SBA-15 (Table 1).

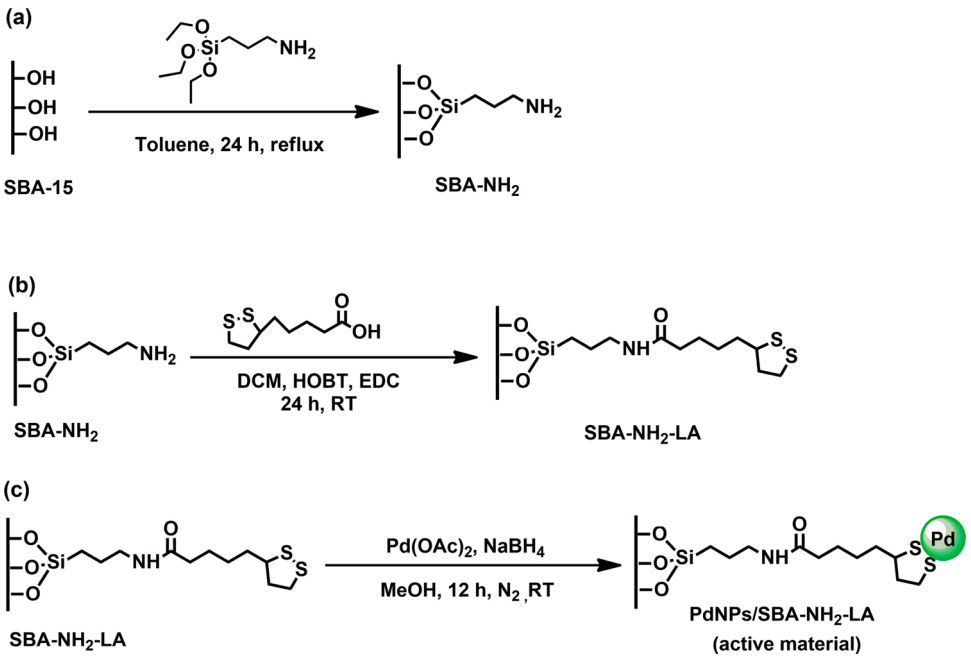

Scheme 2. Schematic representation of PdNPs/SBA-NH_2-LA catalyst.

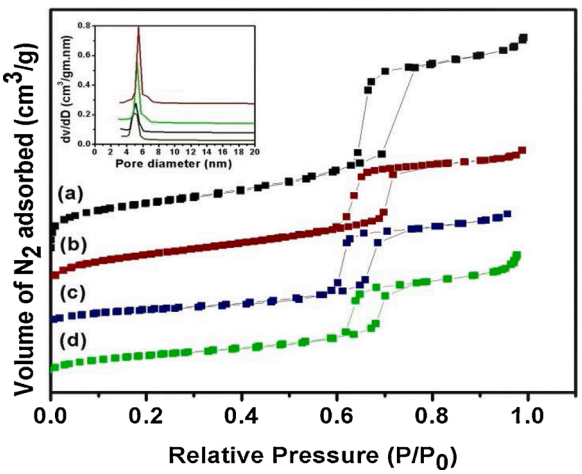

Fig. 1. N_2 adsorption-desorption isotherms of PdNPs/SBA-NH_2-LA samples (a) SBA-15, (b) SBA-NH_2, (c) SBA-NH_2-LA, and (d) PdNPs/SBA-NH_2-LA.

Table 1
Structural and textural properties of SBA-15, SBA-NH_2, SBA-NH_2-LA, and PdNPs/SBA-NH_2-LA.

Catalysts	S_{BET} (m^2/g)[a]	V_t (cm^3/g)[b]	D_{BJH} (nm)[c]	d_{100} (nm)[d]	a_o (nm)[e]	t (nm)[f]
SBA-15	713	1.01	6.99	9.29	10.73	5.63
SBA-NH_2	468	0.87	6.86	8.92	10.30	5.19
SBA-NH_2-LA	429	0.82	6.01	8.83	10.19	5.09
PdNPs/SBA-NH_2-LA	398	0.79	5.98	8.74	10.09	4.99

[a] BET surface area. [b] Total pore volume. [c] BJH pore diameter. [d] d(100) spacing. [e] Unit cell parameter (a_o = 2 x d(100)/$\sqrt{3}$). [f] Pore wall thickness (t = a_o – pore size).

XRD analysis

The low-angle X-ray diffraction analysis of SBA-15, SBA-NH_2, SBA-NH_2-LA, and PdNPs/SBA-NH_2-LA catalysts is shown in Fig. 2. All the catalysts exhibited three well-resolved diffracted peaks. The intense peak at 0.95–1.01° and two weak peaks at 1.67−1.71°, 1.91−1.96° are corresponding to (100), (110), and (200) planes, representing the characteristics of ordered Mesoporous structure. [67] The XRD results suggest that the 2D structure of mesoporous SBA-15 has not been changed during the preparation of the PdNPs/SBA-NH_2-LA catalyst. However, the decrease in the intensity of (100) and (110), (200) planes of SBA-NH_2, SBA-NH_2-LA, and PdNPs/SBA-NH_2-LA might be due to the loss of some uniformity in the 2D hexagonal structure of SBA-15 by filled with propylamine and lipoic acid functional groups.

The wide-angle XRD pattern of the PdNPs/SBA-NH_2-LA catalyst is displayed in Fig. 3. The diffracted peaks observed at 40.11°, 46.74° and 68.1° on the 2θ scale are contributions from (111), (200) and (220) planes of palladium in the metallic state, which is being by the reported values (JCPDS file No.87-0639).

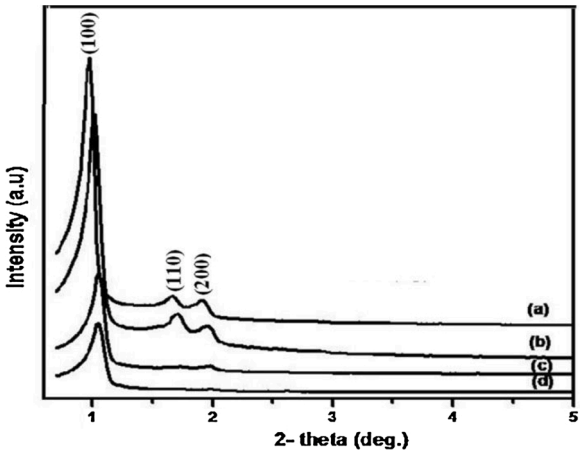

Fig. 2. Low angle XRD pattern of (a) SBA-15, (b) SBA-NH_2, (c) SBA-NH_2-LA, and (d) PdNPs/SBA-NH_2-LA.

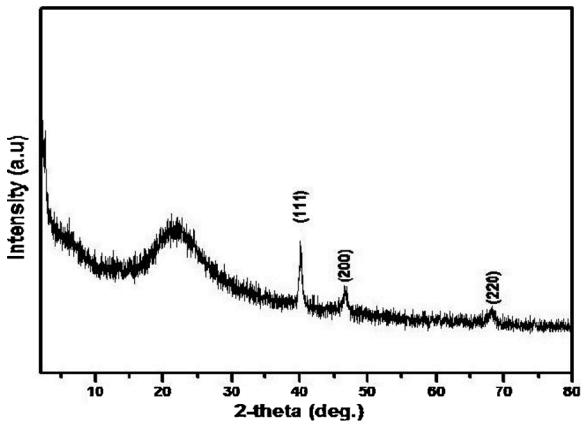

Fig. 3. Wide-angle XRD pattern of PdNPs/SBA-NH_2-LA catalyst.

XPS analysis

XPS analysis has been carried out to determine the oxidation state of Pd in the prepared PdNPs/SBA-NH_2-LA catalyst, and the corresponding spectra is shown in Fig. 4. The survey XPS spectra of PdNPs/SBA-NH_2-LA (Inset, Fig. 4) disclose the presence of Pd, Si, and Oxygen in the catalyst. As shown in Fig. 4, the Pd 3d peak fitted into two peaks, the binding energy at 335.9 eV is attributed to $3d_{5/2}$, and the energy band centered at 342.1 eV is associated with $3d_{3/2}$ of Pd in zero oxidation state. No evidence of Pd^{+2} presence was observed, indicating the palladium is in the reduced form [68] (Fig. 4).

Solid-state 13C CP-MAS NMR analysis

The functionalization of 3-(Aminopropyl)triethoxysilane (APTES) followed by anchoring of lipoic acid on the surface of SBA-15 has been confirmed by solid-state ^{13}C CP-MAS NMR analysis (Fig. 5). As shown in Fig. 5, three peaks observed at 13.2, 24.3, and 45.6 ppm respectively for SBA-NH_2 sample, corresponding to ^{1}C, ^{2}C, and ^{3}C of 3-(Aminopropyl) triethoxysilane (APTES), confirming the immobilization of propylamine group on the surface of SBA-15. [69] After treating of SBA-NH_2 with lipoic acid, the –C = O peak of pure lipoic acid (182 ppm) [70] shifted to 167.5 ppm (SBA-NH_2-LA), representing the amide bond formation between –NH_2 and −COOH groups of SBA-NH_2 and lipoic acid. [70] In addition, SBA-NH_2-LA shows the new peaks in the aliphatic region (10−55 ppm); however, these peaks are merged with the of SBA-NH_2 signals.

FT-IR analysis

Fig. 6 shows the FT-IR spectra of (a) SBA-15, (b) SBA-NH_2 (c) SBA-NH_2-LA. All samples exhibited broadband between 3650−3100 cm^{-1}, which arise from the combination of −OH stretching and intermolecular hydrogen bonding vibrations. New bands appeared in the range of 2937−2860 cm^{-1} and 1494−1383 cm^{-1} for SBA-NH_2 and SBA-NH_2-LA samples, attributed to $-CH_2$ stretching and bending vibrations of anchored propyl amine, lipoic acid groups on the surface of SBA-15. Further, SBA-NH_2 shows the band at 1566 cm^{-1}, which is due to the bending vibration of –NH_2 group. [71,72] Two additional bands appeared for the SBA-NH_2-LA sample at 1520 cm^{-1} and 1648 cm^{-1}, allocated to —C═O stretching frequency in amide (II) group and bending vibrations of –NH group, [55,73] representing the formation amide bond between –NH_2 and −COOH groups of propylamine and lipoic acid on SBA-15.

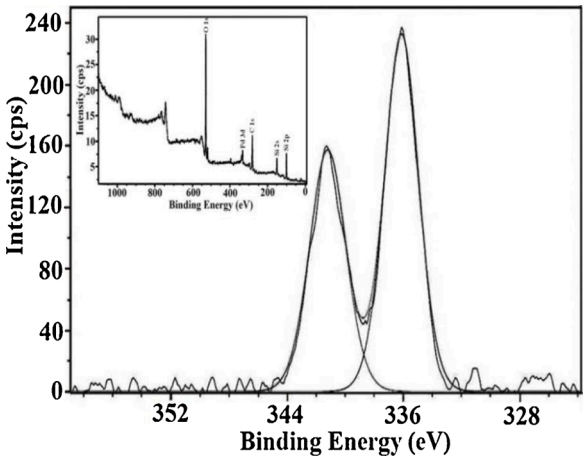

Fig. 4. XPS spectra of PdNPs/SBA-NH_2-LA catalyst.

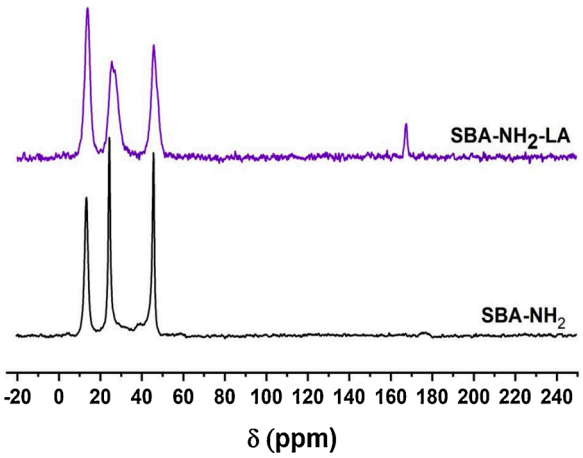

Fig. 5. Solid-state ^{13}C CP-MAS NMR spectra of SBA-NH_2 and SBA-NH_2-LA samples.

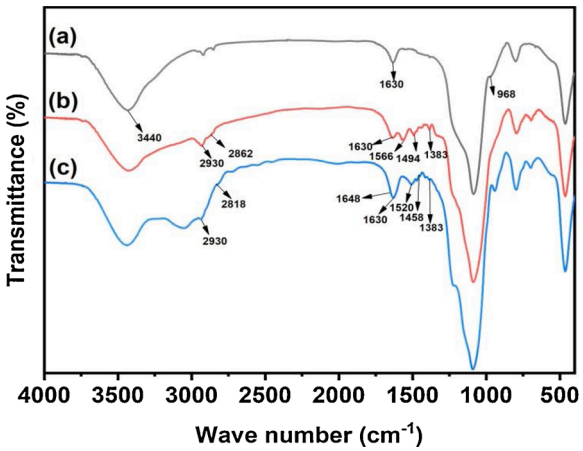

Fig. 6. FT-IR spectra of (a) SBA-15, (b) SBA-NH_2, (c) SBA-NH_2-LA samples.

TEM analysis

The structure and morphology of the PdNPs/SBA-NH_2-LA catalyst were analyzed by TEM analysis, and the corresponding image is shown in Fig. 7. The particle size distribution graph is shown in Fig. 7 as an inset. The TEM analysis results reveal that the Pd nanoparticles are spherical and homogeneously distributed throughout the SBA-15 matrix. The average diameter of Pd nanoparticles determined to be around 12−13 nm with a narrow distribution.

Hydrogenation of C—C double and triple bonds

The catalytic performance of the PdNPs/SBA-NH_2-LA catalyst was

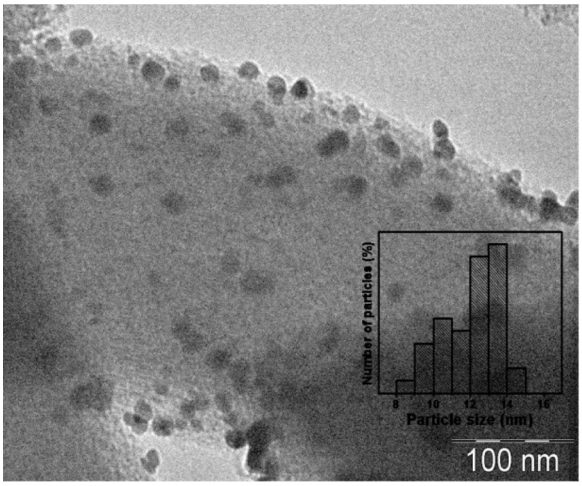

Fig. 7. TEM image of PdNPs/SBA-NH_2-LA catalyst.

evaluated for the selective hydrogenation of C—C double bonds under atmospheric H_2 pressure at room temperature. 1,3-Diphenyl-2-propen-1-one was chosen as a model substrate since it has two different functional groups and easy to monitor the activity and selectivity for the hydrogenation of the C—C double bond over C═O bond. In order to optimize the reaction parameters, the reaction was performed in different solvents, and the results are summarized in Table 2. With non-polar toluene solvent, only 65 % conversion obtained (Table 2, entry 1), while the aprotic polar THF solvent produced 80 % conversion (Table 2, entry 2). Significant improvement in conversion is observed with protic polar methanol and ethanol solvents (85 % and 90 %, Table 2, entry 3,4). Highest conversion (98 %) with 99 % selectivity attained in acetonitrile solvent within 90 min. of reaction time (Table 2, entry 5).

Next, we compare the activity of PdNPs/SBA-NH_2-LA with different catalysts, and the results are shown in Table 3. The reaction did not proceed with parent SBA-15 and SBA-NH_2 (Table 3, entry 1,2), indicating the need for active metal for C—C double bond hydrogenation of 1,3-Diphenyl-2-propen-1-one. Only 25 % conversion with the turn over frequency (TOF) value 92.5 h^{-1} observed with Pd/SBA-15 catalyst (Table 3, entry 3), while the conversion and TOF increased to 53 %, 192.6 h^{-1} when the reaction was performed with SBA-NH_2-Pd catalyst (Table 3, entry 4). The maximum conversion (98 %) and selectivity (99 %) with as high as TOF value were 355 h^{-1} achieved with PdNPs/SBA-NH_2-LA catalyst (Table 3, entry 5) using atmospheric H_2 pressure in acetonitrile solvent at room temperature for 90 min.. The remarkable catalytic activity of the Pd/SBA-NH_2-LA catalyst is due to the formation of small size PdNPs and stabilization of PdNPs through the strong interaction between -SH groups and PdNPs.

Reaction conditions: 1,3-Diphenyl-2-propen-1-one (1 mmol), catalyst (10 mg), acetonitrile (3 mL), 1 atm H_2, room temperature, 90 min. [a]TOF = turnover frequency, moles of product/moles of catalyst (h^{-1})

With the optimized reaction conditions in hand, selective hydrogenation of the C—C double bond of various alkenes with different functional groups was evaluated over Pd/SBA-NH_2-LA catalyst, and the results are depicted in Table 4. Styrene and methyl-substituted styrene underwent complete conversion with excellent selectivity for desired products (Table 4, Entry 1 and 2). When –NH_2 group present on the aromatic ring at *m*-position (Table 4, Entry 3), the reaction took a long time for completion. In the case of 4-Bromostyrene, only double bond was hydrogenated, and no dehalogenated product was observed (Table 4, entry 4). Different aromatic and cyclic α,β-unsaturated compounds were having —C═O, −COOH, and −OH (Table 4, Entry 5–10) functional groups were selectively hydrogenated at C—C double bonds, and the conversions are ranging between 96–99 %. However, these reactions were completed in 90 min. reaction time. The —C═O, −COOH and −OH moieties were untouched during the reaction.

Table 2
Effect of solvent on the hydrogenation of 1,3-Diphenyl-2-propen-1-one over PdNPs/SBA-NH_2-LA catalyst.

Entry	Solvent	Conversion (%)	Selectivity (%)	TOF (h^{-1})
1	Toluene	65	>99	240.7
2	THF	80	>99	296.3
3	Methanol	85	>99	314.8
4	Ethanol	90	>99	333.3
5	Acetonitrile	98	>99	355.0

Reaction conditions: 1, 3-Diphenyl-2-propen-1-on (1 mmol), catalyst (10 mg), solvent (3 mL), 1 atm H_2, room temperature, 90 min.

Table 3
Hydrogenation of 1,3-Diphenyl-2-propen-1-one over different catalysts.

Entry	Catalyst	Time (h)	Conversion (%)	Selectivity (%)	TOF (h^{-1})[a]
1	SBA-15	24	–	–	–
2	SBA-NH2	24	–	–	–
3	Pd/SBA-15	1.5	25	>99	92.6
4	SBA-NH_2-Pd	1.5	53	>99	196.3
5	PdNPs/SBA-NH_2-LA	1.5	98	>99	355.0

Leaching and reusability studies

In order to confirm the no leaching of palladium nanoparticles from PdNPs/SBA-NH_2-LA catalyst, a hot filtration experiment was conducted for the hydrogenation of 1,3-Diphenyl-2-propen-1-one for 1 h under standard reaction conditions (1 mmol 1,3-Diphenyl-2-propen-1-one, 10 mg PdNPs/SBA-NH_2-LA catalyst, 3 mL acetonitrile, 1 atm H_2, room temperature). After 1 h of reaction time, the catalyst was recovered by hot filtration from the reaction mixture. Then, 1 mmol of 1,3-Diphenyl-2-propen-1-one was added to the filtrate and continued the reaction. No further hydrogenation of Diphenyl-2-propen-1-one was observed, demonstrating no leaching of palladium nanoparticles into the solution mixture during the reaction. In addition, the filtrate was further analyzed by ICP-MS analysis and found no traces of palladium nanoparticles in the solution. Evaluate the activity and stability of the used catalyst; the catalyst was collected by simple filtration and washed several times with ethanol solvent. The separated catalyst was dried at room temperature under vacuum and reused five times. The obtained results were displayed in Fig. 8. No significant drop in the activity of the catalyst was noticed as the C—C double bond hydrogenated product was obtained in 96 % yield with 99 % selectivity even after the 5th run. The Pd content in the used catalyst was determined to be 1.94 wt%.

Conclusions

In conclusion, we have prepared a novel PdNPs/SBA-NH_2-LA catalyst by a post-synthetic grafting approach using propylamine (SBA-NH_2) and lipoic acid (SBA-NH_2-LA) functional groups with a particle size of 12−13 nm. This novel catalyst exhibits an excellent activity for chemoselective hydrogenation of C—C double bonds of α, β-unsaturated carbonyl compounds to saturated carbonyl compounds at room temperature under atmospheric hydrogen pressures with high TOF values (330−1065 h^{-1}) Moreover, various functional groups were untouched during the reaction. Moreover, the catalyst is easily recovered and reused five times without losing its activity and selectivity.

Author contribution

Dr. Anand Narani and Dr. David Raju Burri initiated, designed and developed the project. Dr. Anand Narani performed all the experiments

Table 4
Selective hydrogenation of different α,β-unsaturated carbonyl compounds over PdNPs/SBA-NH_2-LA catalyst.

Entry	Reactant	Product	Time (min)	Conversion (%)	Selectivity (%)	[a]TONs	[b]TOF (h^{-1})
1			30	98	>99	532	1065.2
2	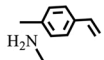	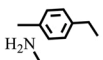	30	99	>99	538	1076
3		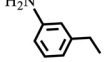	90	96	91	495	329.7
4	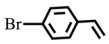	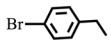	60	96	>99	538	538
5	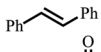	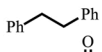	60	99	>99	538	538
6	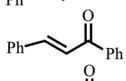	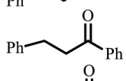	90	98	>99	532	355
7	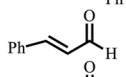	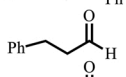	90	98	>99	532	355
8	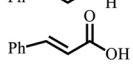	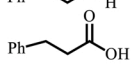	90	96	>99	522	347.8
9	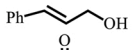	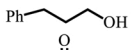	90	96	>99	522	347.8
10			60	97	>99	527	527

Reaction conditions: substrate (1 mmol), catalyst (10 mg), acetonitrile (3 mL), 1 atm H_2, room temperature. TON = turnover number (moles of product/moles of catalyst). [b]TOF = turnover frequency, moles of product/moles of catalyst (h^{-1}).

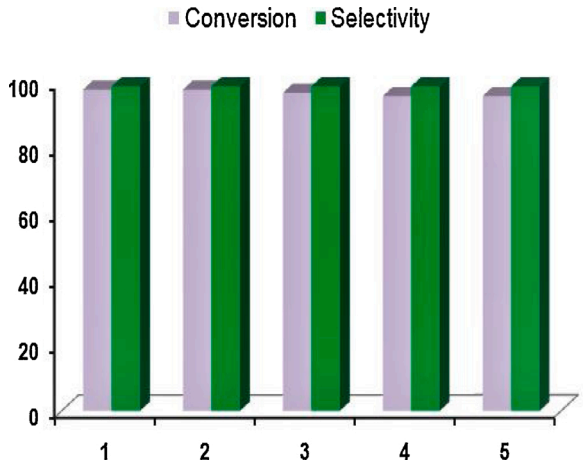

Fig. 8. Reusability of the PdNPs/SBA-NH_2-LA catalyst.

under the supervision of Dr. David Raju Burri, Dr. Kishore Natte and Dr. Hari Prasad Reddy Kannapu corrected the manuscript.

Declaration of Competing Interest

The authors report no declarations of interest.

Acknowledgements

The authors are thanks to CSIR-UGC (INDIA) for financial support. We thank the Director, CSIR-Indian Institute of Petroleum, Dehradun, for his generous support.

References

[1] K. Westerterp, E. Molga, K. van Gelder, Catalytic hydrogenation reactors for the fine chemicals industries; Their design and operation. Heterogeneous catalysis and fine chemicals IV, studies in surface science and catalysis 108, Proceedings 4th International Symposium (1997) 47–57. HU Blaser, A. Baiker and R. Prins.
[2] J. Pritchard, G.A. Filonenko, R. van Putten, E.J. Hensen, E.A. Pidko, Chem. Soc. Rev. 44 (2015) 3808–3833.
[3] K. Murugesan, T. Senthamarai, M. Sohail, A.S. Alshammari, M.-M. Pohl, M. Beller, R.V. Jagadeesh, Chem. Sci. 9 (2018) 8553–8560.
[4] S. Nishimura, Handbook of Heterogeneous Catalytic Hydrogenation for Organic Synthesis, Wiley New York, 2001 etc.
[5] P. Rylander, Catalytic Hydrogenation in Organic Syntheses, Acad, Press, New York, 1979.
[6] H.U. Blaser, C. Malan, B. Pugin, F. Spindler, H. Steiner, M. Studer, Adv. Synth. Catal. 345 (2003) 103–151.
[7] J.G.V. Alsten, M.L. Jorgensen, D.J. am Ende, Org. Process Res. Dev. 13 (2009) 629–633.
[8] P. Clark, M. Poliakoff, A. Wells, Adv. Synth. Catal. 349 (2007) 2655–2659.
[9] M. Rothe, K. Bauer, D. Garbe, Common fragrance and flavour materials. Preparation, properties and uses. 219 Seiten. 450 Einzelkomponenten. VCH Verlagsgesellschaft mbH. Weinheim 1985. Preis: 112,–DM, Food/Nahrung 30 (1986), 228-228.
[10] N. Mamidi, S. Gorai, J. Sahoo, D. Manna, Chem. Phys. Lipids 165 (2012) 320–330.
[11] J.A. VanAllan, G.A. Reynolds, T.H. Regan, J. Org. Chem. 32 (1967) 1897–1899.
[12] M. Kobori, H. Shinmoto, T. Tsushida, K. Shinohara, Cancer Lett. 119 (1997) 207–212.
[13] P. Gallezot, D. Richard, Catal. Rev. 40 (1998) 81–126.
[14] C.A. Mebi, R.P. Nair, B.J. Frost, Organometallics 26 (2007) 429–438.
[15] K. Nuithitikul, M. Winterbottom, Catal. Today 128 (2007) 74–79.
[16] Z. Baán, Z. Finta, G. Keglevich, I. Hermecz, Green Chem. 11 (2009) 1937–1940.
[17] X. Li, L. Li, Y. Tang, L. Zhong, L. Cun, J. Zhu, J. Liao, J. Deng, J. Org. Chem. 75 (2010) 2981–2988.
[18] Z. Poltarzewski, S. Galvagno, R. Pietropaolo, P. Staiti, J.Catal. 102 (1986) 190–198.
[19] W.J. Lu, Y.W. Chen, X.L. Hou, Angew. Chem., Int. Ed. 47 (2008) 10133–10136.
[20] Y. Himeda, N. Onozawa-Komatsuzaki, S. Miyazawa, H. Sugihara, T. Hirose, K. Kasuga, Chem. Eur. J. 14 (2008) 11076–11081.
[21] S. Sakaguchi, T. Yamaga, Y. Ishii, J. Org. Chem. 66 (2001) 4710–4712.
[22] E. Keinan, N. Greenspoon, J. Am. Chem. Soc. 108 (1986) 7314–7325.
[23] B. Ding, Z. Zhang, Y. Liu, M. Sugiya, T. Imamoto, W. Zhang, Org. Lett. 15 (2013) 3690–3693.
[24] D.S. Hays, M. Scholl, G.C. Fu, J. Org. Chem. 61 (1996) 6751–6752.
[25] A.D. Kosal, B.L. Ashfeld, Org. Lett. 12 (2009) 44–47.
[26] E. Keinan, D. Perez, J. Org. Chem. 52 (1987) 2576–2580.
[27] W.S. Mahoney, D.M. Brestensky, J.M. Stryker, J. Am. Chem. Soc. 110 (1988) 291–293.
[28] V. Jurkauskas, J.P. Sadighi, S.L. Buchwald, Org. Lett. 5 (2003) 2417–2420.
[29] M.D. Bhor, A.G. Panda, S.R. Jagtap, B.M. Bhanage, Catal. Lett. 124 (2008) 157–164.
[30] Y. Niu, L.K. Yeung, R.M. Crooks, J. Am. Chem. Soc. 123 (2001) 6840–6846.
[31] S.-S. Lee, B.-K. Park, S.-H. Byeon, F. Chang, H. Kim, Chem. Mater. 18 (2006) 5631–5633.
[32] C. Schmöger, A. Stolle, W. Bonrath, B. Ondruschka, T. Keller, K.D. Jandt, ChemSusChem 2 (2009) 77–82.
[33] A. Stolle, C. Schmoeger, B. Ondruschka, W. Bonrath, T.F. Keller, K.D. Jandt, Chinese J. Catal. 32 (2011) 1312–1322.
[34] D.B. Bagal, B.M. Bhanage, RSC Adv. 4 (2014) 32834–32839.
[35] D.B. Bagal, Z.S. Qureshi, K.P. Dhake, S.R. Khan, B.M. Bhanage, Green Chem. 13 (2011) 1490–1494.

[36] M.L. Kantam, R. Kishore, J. Yadav, M. Sudhakar, A. Venugopal, Adv. Synth. Catal. 354 (2012) 663–669.
[37] S. Ganji, S. Mutyala, C.K.P. Neeli, K.S.R. Rao, D.R. Burri, RSC Adv. 3 (2013) 11533–11538.
[38] S.K. Mahato, R. Ul Islam, C. Acharya, M.J. Witcomb, K. Mallick, ChemCatChem 6 (2014) 1419–1426.
[39] Y. Zhang, X. Yang, Y. Zhou, G. Li, Z. Li, C. Liu, M. Bao, W. Shen, Nanoscale 8 (2016) 18626–18629.
[40] O. Domínguez-Quintero, S. Martínez, Y. Henríquez, L. D'Ornelas, H. Krentzien, J. Osuna, J. Mol. Catal. A Chem. 197 (2003) 185–191.
[41] A. Sharma, V. Kumar, A.K. Sinha, Adv. Synth. Catal. 348 (2006) 354–360.
[42] Z. Baán, Z. Finta, G. Keglevich, I. Hermecz, Tetrahedron Lett. 46 (2005) 6203–6204.
[43] N. Semagina, E. Joannet, S. Parra, E. Sulman, A. Renken, L. Kiwi-Minsker, Appl. Catal. A Gen. 280 (2005) 141–147.
[44] S. Kidambi, M.L. Bruening, Chem. Mater. 17 (2005) 301–307.
[45] M. Zecca, R. Fišera, G. Palma, S. Lora, M. Hronec, M. Králik, Chem. Eur. J. 6 (2000) 1980–1986.
[46] M.-M. Wang, L. He, Y.-M. Liu, Y. Cao, H.-Y. He, K.-N. Fan, Green Chem. 13 (2011) 602–607.
[47] J. Mendes-Burak, B. Ghaffari, C. Copéret, Chem. Commun. 55 (2019) 179–181.
[48] T. Song, Z. Ma, Y. Yang, ChemCatChem 11 (2019) 1313–1319.
[49] T. Suteewong, H. Sai, R. Hovden, D. Muller, M.S. Bradbury, S.M. Gruner, U. Wiesner, Science 340 (2013) 337–341.
[50] E. Doustkhah, H. Mohtasham, M. Hasani, Y. Ide, S. Rostamnia, N. Tsunoji, M.H. N. Assadi, Mol. Catal. 482 (2020), 110676.
[51] D. Zhao, J. Feng, Q. Huo, N. Melosh, G.H. Fredrickson, B.F. Chmelka, G.D. Stucky, Science 279 (1998) 548–552.
[52] M. Choi, W. Heo, F. Kleitz, R. Ryoo, Chem. Commun. (2003) 1340–1341.
[53] Y. Li, A. Chatterjee, L.B. Chen, F.L.-Y. Lam, X. Hu, Mol. Catal. 488 (2020), 110869.
[54] A. Rodríguez-Gómez, F. Platero, A. Caballero, G. Colón, Mol. Catal. 445 (2018) 142–151.
[55] N. Anand, P. Ramudu, K.H.P. Reddy, K.S.R. Rao, B. Jagadeesh, V.S.P. Babu, D. R. Burri, Appl. Catal. A Gen. 454 (2013) 119–126.
[56] A. Narani, R.K. Marella, P. Ramudu, K.S.R. Rao, D.R. Burri, RSC Adv. 4 (2014) 3774–3781.
[57] J. Agúndez, C. Ares, C. Márquez-Álvarez, J. Pérez-Pariente, Mol. Catal. 488 (2020), 110922.
[58] M.M. Islam, P. Bhanja, M. Halder, A. Das, A. Bhaumik, S.M. Islam, Mol. Catal. 475 (2019), 110489.
[59] A. Mohammadkhanni, A. Bazgir, Mol. Catal. 447 (2018) 28–36.
[60] Y. Jia, Z.A. ALOthman, R. Liang, S. Cha, X. Li, W. Ouyang, A. Zheng, S.M. Osman, R. Luque, Y. Sun, Mol. Catal. 495 (2020), 111146.
[61] V. Dufaud, M.E. Davis, J. Am. Chem. Soc. 125 (2003) 9403–9413.
[62] E. Doustkhah, Y. Ide, ACS Appl. Nano Mater. 2 (2019) 7513–7520.
[63] E. Doustkhah, H. Mohtasham, M. Farajzadeh, S. Rostamnia, Y. Wang, H. Arandiyan, M.H.N. Assadi, Microporous Mesoporous Mater. 293 (2020), 109832.
[64] E. Doustkhah, S. Rostamnia, Mater. Chem. Phys. 177 (2016) 229–235.
[65] Q. Hu, J.E. Hampsey, N. Jiang, C. Li, Y. Lu, Chem. Mater. 17 (2005) 1561–1569.
[66] N. Anand, K.H.P. Reddy, V. Swapna, K.S.R. Rao, D.R. Burri, Microporous Mesoporous Mater. 143 (2011) 132–140.
[67] D. Zhao, Q. Huo, J. Feng, B.F. Chmelka, G.D. Stucky, J. Am. Chem. Soc. 120 (1998) 6024–6036.
[68] B. Yuan, Y. Pan, Y. Li, B. Yin, H. Jiang, Angew. Chem., Int. Ed. 49 (2010) 4054–4058.
[69] A.S. Maria Chong, X.S. Zhao, J. Phys. Chem. B 107 (2003) 12650–12657.
[70] L. Maya, G. Muralidharan, T.G. Thundat, E.A. Kenik, Langmuir 16 (2000) 9151–9154.
[71] B. Jarrais, C. Pereira, A.R. Silva, A.P. Carvalho, J. Pires, C. Freire, Polyhedron 28 (2009) 994–1000.
[72] X. Wang, J.C. Chan, Y.-H. Tseng, S. Cheng, Microporous Mesoporous Mater. 95 (2006) 57–65.
[73] H. Sajiki, K. Hattori, K. Hirota, Chem. Eur. J. 6 (2000) 2200–2204.